PCCP

PAPER

View Article Online
View Journal

Cite this: DOI: 10.1039/c7cp08478a

An antibody-free assay for simultaneous capture and detection of glycoproteins by surface enhanced Raman spectroscopy†

D. Xie,‡[ab] W. F. Zhu,‡[a] H. Cheng,[a] Z. Y. Yao, §[a] M. Li *[a] and Y. L. Zhao[ac]

Received 19th December 2017,
Accepted 23rd February 2018

DOI: 10.1039/c7cp08478a

rsc.li/pccp

A sensitive, and single step reaction assay of glycoproteins in antibody-free mode was proposed on a 4-mercapto-phenylboronic acid (4-MPBA) modified silver nanoparticle film (AgNF) by using surface enhanced Raman scattering (SERS). 4-MPBA/AgNF was designed both as a glycoprotein-specific recognition biosensor and as a Raman reporter for the SERS platform. Variation in the ratio I_{1574}/I_{1586} for 4-MPBA/AgNF in response to glycoprotein capture constitutes the SERS assay which exhibits high sensitivity and selectivity against nonglycoproteins and is shown to function in complex samples.

1. Introduction

A glycoprotein is a protein which contains oligosaccharide chains covalently attached to polypeptide side chains. Glycoprotein plays crucial roles in many biological processes, such as molecular recognition, signal transduction, cellular differentiation, immune response, and so on.[1,2] Aberrant expression of glycoproteins is often related to the occurrence and development of diverse diseases.[3] Many glycoproteins are thus used as disease biomarkers for clinical diagnosis.[4,5] For example, α-fetoprotein (AFP) is an oncogenic glycoprotein and an established biomarker for early diagnosis of the most common forms of primary liver cancer.[6–9] The threshold of serum AFP is as low as 20 ng ml^{-1}. A big challenge in current clinical diagnosis is thus the hard collection and detection of trace glycoproteins. Meanwhile a sensitive assay of glycoproteins is significant to revealing the relationship between major cancers and glycoproteins. Though immunoassay is a developed analytical approach for protein analysis, antibodies with high specificity towards target antigens suffer from many disadvantages, like complicated synthesis, high producing cost, poor storage stability and losing activity upon external treatments, *etc.*[10] Besides, antibody-related detections require a complicated, time-consuming method and expensive equipment. In addition, the current antibody cannot differentiate glycoproteins from other proteins effectively. Most importantly, the huge and complicated glycoprotein system makes the development of standard glycoprotein antibody and its further use for disease diagnosis very difficult.[11] Therefore, a robust, sensitive and antibody-free assay of glycoproteins is highly desirable for practical applications.

Boronate-containing materials have become appealing alternatives to antibodies for glycoprotein detection in immunoassays in recent years based on the specific binding reaction between boric acid and glycosyl on glycoproteins.[12–15] The binding ability of *cis*-diol in sugar to boric acid is much stronger than that of dihydroxyl on straight alkane chains (such as ethylene glycol), indicating boronate-containing materials as an ideal sensor for the recognition of sugar-based targets. Assays of glycans based on boronate affinity for glycans exhibit several significant advantages, including broad-spectrum selectivity, reversible covalent binding, temperature- or pH-controlled capture/release,[13] fast association/desorption kinetics, and good compatibility with mass analytical techniques.[16–18]

Among many methods, surface-enhanced Raman scattering (SERS) platforms have shown distinct advantages in biomolecule detection thanks to their transparency in biological environments, and highly sensitive and nondestructive features towards analytes of interest.[19–21] The unique attributes make SERS an ideal tool for biosensing. Many SERS assays of glycoprotein/glycan have been reported on the basis of boronate affinity between boric acid and *cis*-diols. Liu *et al.* introduced an antibody-free boronate affinity sandwich assay for the determination of glycoproteins by using a molecularly imprinted polymer template.[22] Du *et al.* developed a sensitive SERS assay of glycoproteins in combination with Raman reporter-embedded Ag core–Au satellite SERS nanostructures by taking advantage of boronate affinity.[14] A 4-mercaptophenylboronic acid (4-MPBA)-based SERS nanosensor was

[a] CAS Key Laboratory for Biomedical Effects of Nanomaterials & Nanosafety Institute of High Energy Physics, Chinese Academy of Sciences 19B, Yu Quan Road, Beijing 100049, China. E-mail: limin@ihep.ac.cn
[b] Institute of Physical Science and Information Technology, Anhui University, Anhui, 230601, China
[c] CAS Center for Excellence in Nanoscience, National Center for Nanoscience and Technology, Beijing 100190, China

† Electronic supplementary information (ESI) available. See DOI: 10.1039/c7cp08478a

‡ These authors contributed equally to this work.

§ Present address: College of Food Science and Nutritional Engineering, China Agricultural University, Beijing 100083 China.

designed by Liang *et al.* to *in situ* study sialoglycan levels and dynamic expression processes of different cell types based on the boronate affinity between phenylboronic acid and sialoglycans under physiological conditions.[23] Tuncel *et al.* constructed a boronate affinity-assisted SERS tag equipped with a sandwich system to detect glycated hemoglobin in the hemolysate of human erythrocytes.[24] Glycoprotein/glycan assays on the basis of SERS have made great progress. Most of the reported work, however, needs to build a sandwich structure to generate "hot spots" for the Raman signal enhancement. Instead of a single step reaction, a two-step reaction in a typical sandwich assay will affect the total binding efficiency and will no doubt bring more complicated experimental operations, and further complicate the overall sensing mechanism. In this work, glycoprotein detection relies on the reversible change of certain Raman peaks of 4-MPBA upon target recognition on the SERS-active substrate, allowing us to simultaneously capture and detect glycoproteins through a single step reaction.

An antibody-free assay of glycoproteins based on the boronate affinity between glycoproteins and 4-MPBA was constructed on a silver nanoparticle film (AgNF) substrate. The 4-MPBA/AgNF complex serves as both a Raman reporter and a glycoprotein-acceptor due to its large cross section and excellent carbohydrate affinity. Upon coordination to the *cis*-diol parts of glycoproteins, the electronic structure of 4-MPBA/AgNF is affected distinctively, resulting in spectral changes in 4-MPBA/AgNF. Our system offers sensitive detection (limit of detection (LOD) of 10^{-12} M glycoprotein) and rapid response. Finally this system is shown to function well in complex samples. This method may provide a novel exploration for glycoprotein related cancer diagnosis.

2. Experimental section

2.1. Reagents and materials

Silver nitrate ($AgNO_3$), (3-mercaptopropyl)trimethoxysilane (MPTES), glutaraldehyde ($C_5H_8O_2$) and ethylene glycol ($C_2H_6O_2$) were bought from Alfa Aesar. Glucose and 4-MPBA were obtained from Sigma Aldrich. Ethanol (C_2H_6O), sulfuric acid (H_2SO_4), sodium hydroxide (NaOH), ammonium hydroxide solution ($NH_3{\cdot}H_2O$, 30%), hydrogen peroxide solution (H_2O_2, 30%), and methylbenzene ($C_6H_5CH_3$) were purchased from Beijing Chemical Works. Sodium dihydrogen phosphate (NaH_2PO_4) and disodium hydrogen phosphate dodecahydrate (Na_2HPO_4) were obtained from Sinopharm Chemical Reagent Co., Ltd. AFP was purchased from Genway Biotech. All reagents obtained from commercial sources were used without further purification. Triple-distilled water was used throughout the experiment.

2.2. Instrument

All Raman and SERS spectra were recorded on a Thermo Scientific DXR spectrometer equipped with a 780 nm exciting laser (30 mW, 10 μm diameter focal spot laser excitation). SERS spectra were obtained with an acquisition time of 9 s. Samples were kept immersed in PBS solution during SERS measurements. The Raman band of the silicon wafer (111) at 520 cm^{-1} was used to calibrate the spectrometer.

2.3. Preparation of AgNF

AgNF was synthesized following the process reported in our previous work[25] with slight modification. Briefly, glass slides with a size of 0.8 × 1.0 cm^2 were first immersed in ethanol, ultrasonically cleaned for 10 min and dried at 60 °C, then cleaned in piranha solution ($H_2SO_4 : H_2O_2 = 7 : 3$, solution should be handled with great care) for 40 min at 95 °C. After washing with water and ethanol, the slides were immersed in 0.5% MPTES in toluene and incubated for 8 h at room temperature. MPTES modified glass slides were obtained by thoroughly washing the slides with toluene and ethanol, respectively, and stored in water for further use.

To prepare silver nanoparticles, 440 mg of silver nitrate was dissolved in 50 ml of water and 135 μl of NaOH (10%) was added dropwise to form a brownish suspension. Following that, a 10% ammonia solution was added dropwise till the suspension turned transparent again. After cooling down in an ice-water bath, 300 μl of glutaraldehyde (25%) was added quickly to the solution and stirred for 10 s. The resulting mixture was transferred to a 90 °C water bath with MPTES modified glass slides hanging in it. After incubation for 4 min, the glass sides were transferred to pre-cooled ethylene glycol and AgNF was obtained after sonication for 20 s.

2.4. Preparation of the SERS probe

4-MPBA was dissolved in ethanol to a concentration of 1 mM. AgNF was immersed in 4-MPBA (1 mM) solution for 3 h at room temperature for covalently binding 4-MPBA to Ag substrates. After thoroughly rinsing with ethanol and PBS, a glycoprotein SERS probe was obtained. The SERS spectra of the probes were recorded with the substrates being kept immersed in PBS (10 mM, pH 7.4).

2.5. Simultaneous capturing and sensing of glycoproteins

To prove the feasibility of our approach, glucose was tested first. Briefly, 4-MPBA modified AgNF was incubated with different glucose concentrations in PBS for 1 h. For glycoprotein detection, AFP (0.05 ng ml^{-1}, 0.5 ng ml^{-1}, 5 ng ml^{-1}, 50 ng ml^{-1}, 500 ng ml^{-1}) was added instead while keeping other conditions the same.

2.6. Capture and release of glycoproteins

To demonstrate the reversible reaction ability of 4-MPBA, capture and release of glucose was performed and monitored on 4-MPBA modified AgNF according to the following procedure. Firstly, 4-MPBA modified AgNF was incubated with 10^{-2} M glucose in PBS for 1 h to effectively capture glucose. After that, AgNF was taken out and immersed in pure PBS for 1 h to release glucose. The reversible reaction was surveyed by monitoring the variation in the ratio I_{1574}/I_{1586}.

3. Results and discussion

The principle of an antibody-free assay of glycoproteins is presented in Scheme 1. 4-MPBA was chemisorbed to the freshly prepared AgNF through the reaction between –SH and Ag to form 4-MPBA/AgNF. The SERS spectrum of 4-MPBA was recorded and the main peaks were labeled as I_1 and I_2. 4-MPBA is known to be able to react with the carbohydrate moieties on glycoproteins

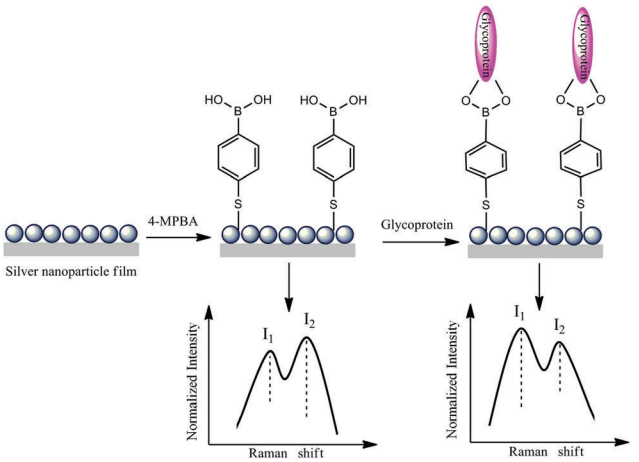

Scheme 1 Schematic illustration of an antibody-free assay of glycoproteins based on boronate affinity reaction between 4-MPBA and AFP.

to form cyclic boronate esters with 1,2- or 1,3-diols under certain conditions.[26] According to our previous work,[25] it is expected that binding of different amounts of glycoproteins would result in varying degrees of electron distribution for 4-MPBA/AgNF, which can be reflected from the variation in the ratio I_1/I_2 of 4-MPBA/AgNF.

Fig. 1A shows a typical SEM image of the as-prepared AgNF used for SERS measurement on a glass substrate. It is clearly seen that the AgNPs are densely decorated on the glass slide with a diameter of Ag particles of ~38 nm (Fig. 1B), which is very conducive for Raman enhancement. The SERS spectrum of 4-MPBA/AgNF is presented in Fig. 1C along with the spectra of the bare silver nanoparticle film and glycoprotein bound 4-MPBA/AgNF. The five dominant peaks at 1586, 1574, 1074, 1022, and 998 cm^{-1} are ascribed to totally symmetric (8a) vibrational modes of the benzene ring, nontotally symmetric (8b) vibrational modes of the benzene ring,[27] C–C in-plane bending coupled with C–S stretching,[28] C–H in-plane bending as well as B–O–H deformation vibration,[29] respectively. After binding with glycoproteins, the peak ratio of I_{1574}/I_{1586} reversed as shown in Fig. 1C. The symmetry breaking of the 4-MPBA molecule upon glycoprotein binding accounts for the ratio variation between totally (8a) and nontotally (8b) symmetric ring vibration modes (the peaks at 1586 cm^{-1} and 1574 cm^{-1}, respectively) due to Herzberg–Teller contributions as shown in Fig. 1D.[30] These assignments correspond well with the previous reports[24,31] and are also listed in Table S1 (ESI†).

The SERS spectral modality of 4-MPBA/AgNF shows a subtle difference when measured in aqueous solutions with different pH values due to its hydrolysis.[32] Under the acidic conditions, 4-MPBA is hard to hydrolyze and tends to adopt a tilted orientation instead of standing perpendicular to the surface of Ag nanoparticles. Hydrolysis is prone to occur and form OH^- – associated 4-MPBA when pH > 7.0. However, OH^- – associated 4-MPBA likely forms trimers *via* the self-condensation process under strong alkaline conditions.[33] Meanwhile, hydrolysis somehow would facilitate the formation of cyclic boronate esters between boronic acid and 1,2- or 1,3-diols.[34] Therefore, to avoid the self-condensation of 4-MPBA and considering the physiological requirements, pH 7.4 was chosen as the appropriate condition for the whole experiments.

Fig. 2A shows the Raman spectra of 4-MPBA in powder (red curve) and in PBS 7.4 solution (black curve). The dominant peak at 1600 cm^{-1} for 4-MPBA in the powder state was split into two peaks for 4-MPBA/AgNF at 1574 cm^{-1} and 1586 cm^{-1}, respectively, which accounts for the electronic structure change of 4-MPBA/AgNF either after hydrolysis[33] or after the formation of the cyclic boronate ester.[35–37] In the latter case, the intensity ratios of 1574 cm^{-1} and 1586 cm^{-1} peaks (I_{1574}/I_{1586}) were used to monitor glycoprotein recognition. It should be noted that a laser wavelength of 780 nm and a power of 30 mW were employed in the whole measurements to avoid the possible deboronation reaction of 4-MPBA when binding with glucose/glycoprotein on silver surfaces,[38] and the exposure time for spectra collection was limited to 9 s. Fig. 2B shows the extinction spectra of the silver nanoparticle film before and after AFP binding to the 4-MPBA/AgNF substrate. The plasmon resonance peak originally at 483 nm for the Ag film shifts to red by 14 nm after binding to 4-MPBA and further by 7.5 nm after treatment

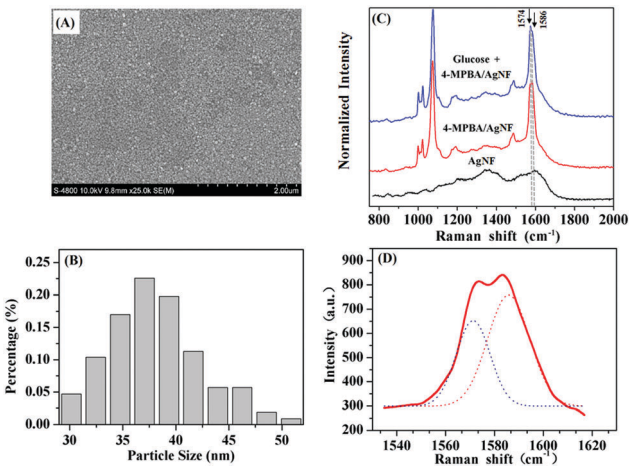

Fig. 1 (A) SEM image of the as-prepared AgNF; (B) Ag nanoparticles size distribution derived from the square in (A); (C) SERS spectrum of Ag nanoparticle films (blank curve), 4-MPBA/AgNF (red curve) and glucose-4-MPBA/AgNF (blue curve); (D) simulation spectra of the 8a and 8b vibration modes of 4-MPBA/AgNF in (C).

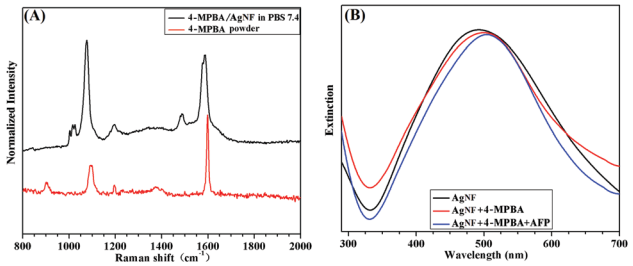

Fig. 2 (A)SERS spectra of the 4-MPBA powder and 4-MPBA/AgNF in PBS 7.4. (B) Extinction spectra of a less dense Ag nanopartical film (black curve) showing the shifts in the plasmon resonance peak at 483 nm upon binding with 4-MPBA (red curve) and then with AFP (blue curve).

with 10^{-8} M glycoprotein(AFP) solution. This shift is attributed to the modification of the refractive index for silver nanoparticle substrates by the binding moieties.

The cyclic boronate ester reaction between boronic acid and 1,2- or 1,3-diols is known to be reversible. To assess this, glucose with 10^{-2} mM concentration was firstly captured by covalently binding to the 4-MPBA/AgNF film, then the glucose-4-MPBA/AgNF film was immersed in PBS buffer (pH 7.4, 1 h) for glucose release within the first cycle. It is clearly shown that glucose can largely release within one cycle from the spectral modality as shown in Fig. 3A. The ratio variation of I_{1574}/I_{1586} in Fig. 3A is extracted and presented in Fig. 3B. Meanwhile, it should be noted that the value of I_{1574}/I_{1586} can be subtly different for the parallel measurements at different substrates as shown in Fig. 3B (black column), which could be due to the high spectral sensitivity of hydrolyzed 4-MPBA to the highly faceted silver nanoparticles at pH 7.4. Since the capture and release of glycoproteins is also closely related to temperature,[13] performing the whole experiments under fixed temperature conditions is crucial to the objectivity of the results. The temperature effect on the blank of the 4-MPBA/AgNF substrate in pH 7.4 buffer is clearly shown in Fig. S1 (ESI†). It is worth noting that temperature could also affect the release efficiency, which will be revealed in future work. Considering that 4-MPBA hydrolysis also contributes to the variation in the ratio I_{1574}/I_{1586}, performing all measurements on one substrate for glycoprotein detection eliminates any major errors caused by different 4-MPBA/AgNF films and meanwhile strictly controls the pH value.

Prior to glycoprotein detection, the sensing performance of the 4-MPBA/AgNF films towards glucose was tested firstly after incubation of 4-MPBA/AgNF films with glucose solution of various concentrations. With the increase of glucose concentrations, distinct changes in the intensity of normalized SERS spectra of 4-MPBA/AgNF films were observed as shown in Fig. 4A, including increases in the band intensities at 999 cm^{-1} and 1022 cm^{-1} when the spectra are normalized to the intensity of the band at 1074 cm^{-1} (ν(CS)). The pronounced intensity change of the spectra at the peaks of 1574 cm^{-1} and 1586 cm^{-1} is shown more clearly in Fig. 4B. The peak intensity at 1574 cm^{-1} ascribed to 8b mode vibrations of 4-MPBA increases gradually while the peak intensity at 1586 cm^{-1} to the 8a mode vibrations decreases with the increase in glucose concentration. The peak ratio I_{1574}/I_{1586} is

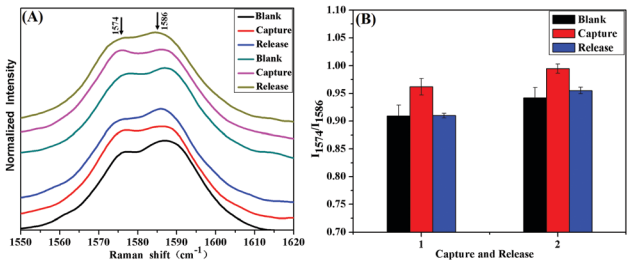

Fig. 3 (A) SERS spectra of glucose capture and release to 4-MPBA/AgNF. (B) The reversal reaction between glucose and 4-MPBA/AgNF confirmed by the spectral change of I_{1574}/I_{1586} at 10^{-2} M glucose solution. Error bars indicate the standard deviation of 3 repeated measurements.

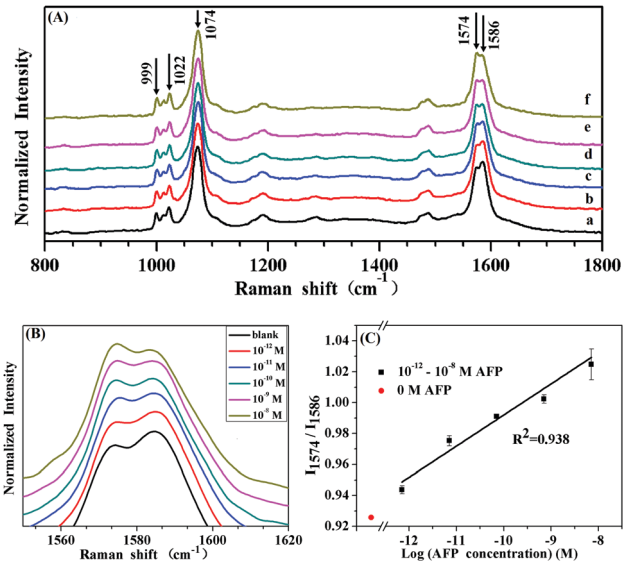

Fig. 4 (A) Typical SERS spectra of 4-MPBA for the detection of different concentrations of glucose, 0, 10^{-5}, 10^{-4}, 5×10^{-4}, 10^{-3}, 5×10^{-3} and 10^{-2} M from (a to g), respectively. (B) Details of the spectral region in 1545–1620 cm^{-1} (C) Plot of the value of I_{1574}/I_{1586} *vs.* glucose concentrations. Error bars indicate the standard deviation of 3 repeated measurements.

found to be quantitatively correlated with the glucose concentration as shown in Fig. 4C. Clearly, the I_{1574}/I_{1586} value increases linearly in the range of 10^{-5}–10^{-2} M glucose, with a LOD of 10^{-5} M. The results show that the SERS spectra of 4-MPBA/AgNF films can be used for the quantitative detection of glucose in aqueous solution.

To examine the performance of 4-MPBA/AgNF films, AFP was employed here as a model glycoprotein. Fig. 5A shows the Raman spectra of 4-MPBA/AgNF after treatment with AFP PBS

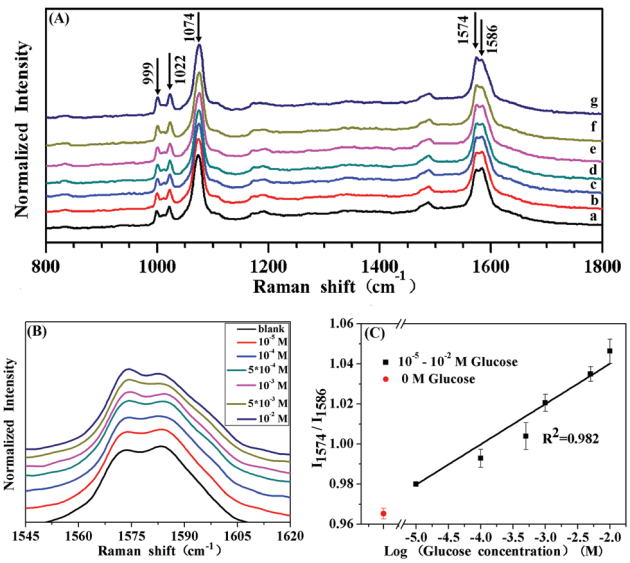

Fig. 5 (A) SERS spectra of 4-MPBA for the detection of different concentrations of AFP, 0, 10^{-12}, 10^{-11}, 10^{-10}, 10^{-9} and 10^{-8} M from (a to g), respectively. (B) Details of the spectral region 800–1800 cm^{-1}. (C) Semi-log plot of I_{1574}/I_{1586} as a function of AFP concentration. Error bars indicate the standard deviation of 3 repeated measurements.

solution in the range of 10^{-12} to 10^{-8} M concentrations. The spectral changes of 4-MPBA/AgNF in 8a and 8b vibration modes were also observed upon AFP recognition. A more detailed peak intensity variation (I_{1574}/I_{1586}) is presented in Fig. 5B. When increasing AFP concentrations, the peak intensity at 1574 cm^{-1} and 1586 cm^{-1} reverses gradually, indicating the successful AFP capture by the 4-MPBA/AgNF film. The plot of the I_{1574}/I_{1586} ratio *versus* log AFP concentration is linear over the range of 10^{-12}–10^{-8} M AFP, indicating a quantitative detection of glycoproteins (Fig. 5C). Considering 3 times the blank uncertainty to define the LOD for the sensor, 10^{-12} M is claimed as a conservative LOD for the AFP assay, suggesting the high sensitivity of our sensing platform for glycoprotein detection.

To evaluate the selectivity of this glycoprotein antibody-free sensor, both BSA (nonglycoprotein) and AFP were tested for comparison after exposing the 4-MPBA/AgNF film to 500 ng ml^{-1} BAS and AFP spiked solution, respectively. It is clearly shown in Fig. 6A and B that the nonglycoprotein had only subtle effects on the 4-MPBA/AgNF Raman spectrum even at a very high concentration (500 ng ml^{-1}) since boronate affinity couldn't occur between 4-MPBA and the nonglycoprotein which doesn't contain carbohydrate moieties (black and red curves in Fig. 6A). A prominent response is only observed in the presence of glycoproteins (green curve in Fig. 6A), AFP.

Further experiments on the AFP concentration dependency were performed in a complex sample solution spiked with the same amount of BSA as the interfering substance. The plot curve is shown in Fig. 6C. A good linear relationship was obtained between the I_{1574}/I_{1586} ratio and the log concentration of AFP (R^2 = 0.978, from 10^{-12} M to 10^{-8} M). It should be noted that the slope of this plot is slightly smaller than that for pure AFP measurements (Fig. 5C), possibly due to the interference of a large amount of BSA in the vicinity (50% in mass concentration). The LOD was determined to be 10^{-12} M, confirming the high selectively of this assay over nonglycoproteins.

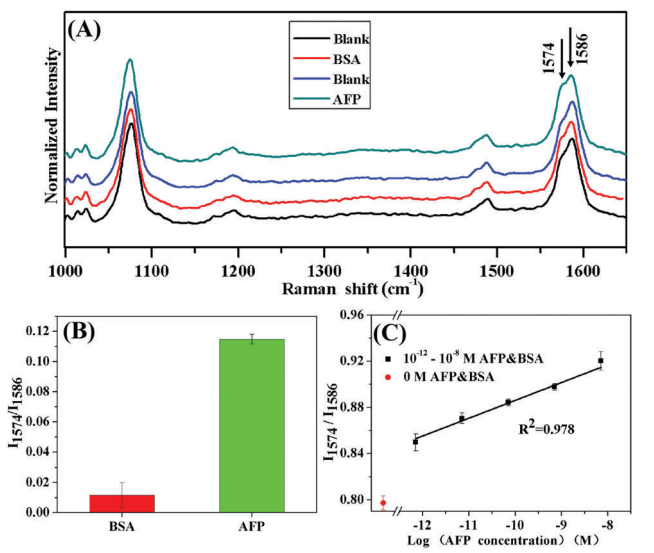

Fig. 6 (A) Normalized SERS spectra of 4-MPBA/AgNF in the presence of BSA and AFP, respectively. (B) The comparison of the I_{1574}/I_{1586} value for 4-MPBA/AgNF exposure to 10 mM PBS solutions containing 500 ng ml^{-1} BSA and AFP, respectively. (C) Semi-log plot of I_{1574}/I_{1586} as a function of AFP and BSA concentration. Error bars indicate the standard deviation of 3 repeated measurements.

4. Conclusions

In conclusion, we have developed a sensitive, antibody-free assay for simultaneous capture and detection of glycoproteins based on the Raman spectral changes of 4-MPBA/AgNF upon glycoprotein binding. We find picomolar sensitivity and high selectivity of glycoproteins over nonglycoproteins in PBS buffer solution. The assay maintains its sensitivity and selectivity in complex samples with spiked equal amounts of AFP and BSA. This work shows high potential for sensitive detection of glycoproteins in clinical settings using SERS spectroscopy.

Conflicts of interest

There are no conflicts to declare.

Acknowledgements

This work was supported by the National Natural Science Foundation of China (grant no. 31671012), and the National Basic Research Program of China (no. 2015CB932004).

Notes and references

1 P. M. Rudd, T. Elliott, P. Cresswell, I. A. Wilson and R. A. Dwek, *Science*, 2001, **291**, 2370–2376.
2 G. Walsh and R. Jefferis, *Nat. Biotechnol.*, 2006, **24**, 1241–1252.
3 J. Munkley and D. J. Elliott, *Oncotarget*, 2016, **7**, 35478–35489.
4 A. Flyvbjerg, *Nat. Rev. Nephrol.*, 2017, **13**, 311–318.
5 M. Yamamoto, T. Takahashi, S. Serada, T. Sugase, K. Tanaka, Y. Miyazaki, T. Makino, Y. Kurokawa, M. Yamasaki, K. Nakajima, S. Takiguchi, T. Naka, M. Mori and Y. Doki, *Cancer Sci.*, 2017, **108**, 2052–2060.
6 A. Arzumanyan, H. M. G. P. V. Reis and M. A. Feitelson, *Nat. Rev. Cancer*, 2013, **13**, 123–135.
7 A. S. Lok, R. K. Sterling, J. E. Everhart, E. C. Wright, J. C. Hoefs, A. M. Dibisceglie, T. R. Morgan, H. Y. Kim, W. M. Lee, H. L. Bonkovsky and J. L. Dienstag, *Gastroenterology*, 2010, **138**, 493–502.
8 J. P. Yu, X. G. Xu, R. J. Ma, S. N. Qin, C. R. Wang, X. B. Wang, M. Li, M. S. Li, Q. Ma and W. W. Xu, *J. Clin. Lab. Anal.*, 2015, **29**, 85–93.
9 M. Biselli, F. Conti, A. Gramenzi, M. Frigerio, A. Cucchetti, G. Fatti, M. D'Angelo, M. D. Agata, E. G. Giannini, F. Farinati, F. Ciccarese, P. Andreone, M. Bernardi and F. Trevisani, *Br. J. Cancer*, 2015, **112**, 69–76.
10 T. Shi, T. L. Fillmore, X. F. Sun, R. Zhao, A. A. Schepmoes, M. Hossain, F. Xie, S. Wu, J. S. Kim, N. Jones, R. J. Moore, L. Paša-Tolic, J. Kagan, K. D. Rodland, T. Liu, K. Tang,

D. G. Camp, R. D. Smith and W. J. Qian, *Proc. Natl. Acad. Sci. U. S. A.*, 2012, **109**, 15395–15400.
11 L. Pan, H. A. Aguilar, L. Wang, A. Lliuk and W. A. Tao, *J. Am. Chem. Soc.*, 2016, **138**, 15311–15314.
12 L. Li, Y. Lu, Z. J. Bie, H. Y. Chen and Z. Liu, *Angew. Chem., Int. Ed.*, 2013, **52**, 7451–7454.
13 W. Zhang, W. Liu, P. Li, H. Xiao, H. Wang and B. Tang, *Angew. Chem.*, 2014, **126**, 12697–12701.
14 X. S. Bi, X. Y. Li, D. Chen and X. Z. Du, *ACS Appl. Mater. Interfaces*, 2016, **8**, 10683–10689.
15 X. Y. Tu, P. Muhammad, J. Liu, Y. Y. Ma, S. S. Wang, D. Y. Yin and Z. Liu, *Anal. Chem.*, 2016, **88**, 12363–12370.
16 W. L. Zhai, X. L. Sun, T. D. James and J. S. Fossey, *Chem. – Asian J.*, 2015, **10**, 1836–1848.
17 H. Torul, H. Çiftçi, F. C. Dudak, Y. Adıgüzel, H. Kulah, İ. H. Boyacı and U. Tamer, *Anal. Methods*, 2014, **6**, 5097–5104.
18 X. C. Sun, S. Stagon, H. C. Huang, J. Chen and Y. Lei, *RSC Adv.*, 2014, **4**, 23382–23388.
19 A. Samanta, K. K. Maiti, K. S. Soh, X. J. Liao, M. Vendrell, U. S. Dinish, S. W. Yun, R. Bhuvaneswari, H. Kim, S. Rautela, J. H. Chung, M. Olivo and Y. T. Chang, *Angew. Chem., Int. Ed.*, 2011, **50**, 6089–6092.
20 Y. F. Yuan, Y. Lin, B. Gu, N. Panwar, S. C. Tjin, J. Song, J. L. Qu and K. T. Yong, *Coord. Chem. Rev.*, 2017, **339**, 138–152.
21 S. Laing, L. E. Jamieson, K. Faulds and D. Graham, *Nat. Rev. Chem.*, 2017, **1**, 60.
22 J. Ye, Y. Chen and Z. Liu, *Angew. Chem., Int. Ed.*, 2014, **53**, 10386–10389.
23 L. J. Liang, H. X. Qu, B. Y. Zhang, J. Zhang, R. Deng, Y. T. Shen, S. P. Xu, C. Y. Liang and W. Q. Xu, *Biosens. Bioelectron.*, 2017, **94**, 148–154.
24 D. D. Usta, K. Salimi, A. Pinar, İ. Coban, T. Tekinay and A. Tuncel, *ACS Appl. Mater. Interfaces*, 2016, **8**, 11934–11944.
25 B. C. Tang, J. J. Wang, J. A. Hutchison, L. Ma, N. Zhang, H. Guo, Z. B. Hu, M. Li and Y. L. Zhao, *ACS Nano*, 2016, **10**, 871–879.
26 B. Preinerstorfer, M. Lämmerhofer and W. Lindner, *J. Sep. Sci.*, 2009, **32**, 1673–1685.
27 F. Sun, T. Bai, L. Zhang, J. R. E. Menye, S. J. Liu, A. K. Nowinski, S. Y. Jiang and Q. M. Yu, *Anal. Chem.*, 2014, **86**, 2387–2394.
28 D. S. Grubisha, R. J. Lipert, H. Y. Park, J. Driskell and M. D. Porter, *Anal. Chem.*, 2003, **75**, 5936–5943.
29 Y. Erdogdu, M. T. Güllüoğlu and M. Kurt, *J. Raman Spectrosc.*, 2009, **40**, 1615–1623.
30 J. R. Lombardi, R. L. Birke, T. Lu and J. Xu, *J. Chem. Phys.*, 1986, **84**, 4174–4180.
31 M. Tabatabaei, G. Q. Wallace, F. A. Caetano, E. R. Gillies, S. S. G. Ferguson and F. L. Labarthet, *Chem. Sci.*, 2016, **7**, 575–582.
32 S. S. Li, Q. Zhou, W. Y. Chu, W. Zhao and J. W. Zheng, *Phys. Chem. Chem. Phys.*, 2015, **17**, 17638.
33 H. Su, Y. Wang, Z. Yu, Y. Liu, X. L. Zhang, X. L. Wang, H. Sui, C. B. Sun and B. Zhao, *Spectrochim. Acta, Part A*, 2017, **185**, 336–342.
34 T. D. James and S. Shinkai, *Top. Curr. Chem.*, 2002, **218**, 159–200.
35 T. V. Shishkanova, V. Král, P. Fitl, M. Vrňata and P. Matějka, *Electroanalysis*, 2015, **27**, 713–719.
36 S. Takahashi and J. I. Anzai, *Langmuir*, 2005, **21**, 5102–5107.
37 P. Gao and M. J. Weaver, *J. Phys. Chem.*, 1985, **89**, 5040–5046.
38 N. H. Ly, A. T. N. Lam, D. B. Nguyen, Y. J. Kwark and S. W. Joo, *Surf. Interface Anal.*, 2017, **49**, 495–502.

